Complex of a Protective Antibody with Its Ebola Virus GP Peptide Epitope: Unusual Features of a Vλ$_x$ Light Chain

Jeffrey E. Lee[1], Ana Kuehne[2], Dafna M. Abelson[1], Marnie L. Fusco[1], Mary Kate Hart[2] and Erica Ollmann Saphire[1]*

[1]*Department of Immunology, The Scripps Research Institute, 10550 North Torrey Pines Road, La Jolla, CA 92037, USA*

[2]*Virology Division, U.S. Army Medical Research Institute of Infectious Diseases, 1425 Porter Street, Fort Detrick, Frederick, MD 21702, USA*

13F6-1-2 is a murine monoclonal antibody that recognizes the heavily glycosylated mucin-like domain of the Ebola virus virion-attached glycoprotein (GP) and protects animals against lethal viral challenge. Here we present the crystal structure, at 2.0 Å, of 13F6-1-2 in complex with its Ebola virus GP peptide epitope. The GP peptide binds in an extended conformation, anchored primarily by interactions with the heavy chain. Two GP residues, Gln P406 and Arg P409, make extensive side-chain hydrogen bond and electrostatic interactions with the antibody and are likely critical for recognition and affinity. The 13F6-1-2 antibody utilizes a rare Vλ$_x$ light chain. The three light-chain complementarity-determining regions do not adopt canonical conformations and represent new classes of structures distinct from Vκ and other Vλ light chains. In addition, although Vλ$_x$ had been thought to confer specificity, all light-chain contacts are mediated through germ-line-encoded residues. This structure of an antibody that protects against the Ebola virus now provides a framework for humanization and development of a postexposure immunotherapeutic.

Edited by M. Guss

Introduction

The Ebola virus causes a severe hemorrhagic fever usually involving uncontrolled viral replication, multiple organ failure, and death 6–9 days after onset of symptoms.[1] The 13 known outbreaks between 1976 and 2004 have resulted in 50–90% fatality[2] with the highest lethality associated with the Zaire subtype of the virus.[3,4]

Corresponding author. E-mail address: erica@scripps.edu.
Present address: M. K. Hart, DynPort Vaccine Company (DVC) LLC, a CSC Company, 64 Thomas Johnson Drive, Frederick, MD 21702, USA.

Abbreviations used: CDR, complementarity-determining region; mAb, monoclonal antibody; GP, glycoprotein; sGP, secreted glycoprotein; IgG, immunoglobulin G; V$_H$, variable heavy chain; V$_L$, variable light chain; TCR, T-cell receptors; PBS, phosphate-buffered saline; BSA, bovine serum albumin; TBS, Tris-buffered saline.

An interesting feature of the Ebola virus genome is its ability to encode separate glycoproteins, which share 295 amino acids of N-terminal sequence, but have unique C-termini, which lead to different patterns of disulfide bonding and different structures. The primary gene product is a small, dimeric glycoprotein called secreted glycoprotein (sGP, 364 amino acids), which is shed abundantly from infected cells. The secondary gene product is a larger glycoprotein called GP (676 amino acids),[5] which is proteolytically cleaved into two subunits (GP1 and GP2) connected by a disulfide linkage. Three GP1–GP2 units form a trimeric, transmembrane envelope spike, which is the sole protein expressed on the surface of the Ebola virus and is involved in receptor binding, tropism, and viral entry.[6–9]

It will be desirable to have well-characterized, effective immunotherapeutics against the Ebola virus available in case of exposure, outbreak, or release of the virus. Several monoclonal antibodies (mAbs) have demonstrated protection against the

Report Documentation Page			*Form Approved* *OMB No. 0704-0188*

Public reporting burden for the collection of information is estimated to average 1 hour per response, including the time for reviewing instructions, searching existing data sources, gathering and maintaining the data needed, and completing and reviewing the collection of information. Send comments regarding this burden estimate or any other aspect of this collection of information, including suggestions for reducing this burden, to Washington Headquarters Services, Directorate for Information Operations and Reports, 1215 Jefferson Davis Highway, Suite 1204, Arlington VA 22202-4302. Respondents should be aware that notwithstanding any other provision of law, no person shall be subject to a penalty for failing to comply with a collection of information if it does not display a currently valid OMB control number.

1. REPORT DATE **4 JAN 2008**	2. REPORT TYPE **N/A**	3. DATES COVERED

4. TITLE AND SUBTITLE **Complex of a protective antibody with its Ebola virus GP peptide epitope: unusual features of a Vλx light chain. Journal of Molecular Biology 375:202-216**	5a. CONTRACT NUMBER
	5b. GRANT NUMBER
	5c. PROGRAM ELEMENT NUMBER
6. AUTHOR(S) **Lee /JE Kuehne, A Abelson, DM Fusco, ML Hart, MK Saphire, EO**	5d. PROJECT NUMBER
	5e. TASK NUMBER
	5f. WORK UNIT NUMBER
7. PERFORMING ORGANIZATION NAME(S) AND ADDRESS(ES) **United States Army Medical Research Institute of Infectious Diseases, Fort Detrick, MD**	8. PERFORMING ORGANIZATION REPORT NUMBER **TR-07-058**
9. SPONSORING/MONITORING AGENCY NAME(S) AND ADDRESS(ES)	10. SPONSOR/MONITOR'S ACRONYM(S)
	11. SPONSOR/MONITOR'S REPORT NUMBER(S)

12. DISTRIBUTION/AVAILABILITY STATEMENT
Approved for public release, distribution unlimited.

13. SUPPLEMENTARY NOTES
The original document contains color images.

14. ABSTRACT
13F6-1-2 is a murine monoclonal antibody that recognizes the heavily glycosylated mucin-like domain of the Ebola virus virion-attached glycoprotein (GP) and protects animals against lethal viral challenge. Here we present the crystal structure, at 2.0 Å, of 13F6-1-2 in complex with its Ebola virus GP peptide epitope. The GP peptide binds in an extended conformation, anchored primarily by interactions to the heavy chain. Two GP residues, Gln P406 and Arg P409, make extensive side-chain H-bond and electrostatic interactions to the antibody and are likely critical for recognition and affinity. The 13F6-1-2 antibody utilizes a rare Vλx light chain. Surprisingly, the three CDR light chain loops do not adopt canonical conformations and represent new classes of structures distinct from Vλ and Vκ light chains. The light chain makes five hydrogen bonds to the peptide, but interestingly, all contacts are mediated through germ line-encoded residues. The 13F6-1-2 Vλx light chain shares strong sequence identity to human Vλ subgroup VIII, thus providing a framework for humanization. This first structure of a Vx light chain and Ebola virus-neutralizing antibody is an exciting step towards the development of a postexposure therapeutic antibody.

15. SUBJECT TERMS

16. SECURITY CLASSIFICATION OF:			17. LIMITATION OF ABSTRACT	18. NUMBER OF PAGES	19a. NAME OF RESPONSIBLE PERSON
a. REPORT **unclassified**	b. ABSTRACT **unclassified**	c. THIS PAGE **unclassified**	**SAR**	**15**	

Standard Form 298 (Rev. 8-98)
Prescribed by ANSI Std Z39-18

Ebola virus in rodent models[10–12]; one mAb failed to protect in a macaque model.[13] It is as yet unclear whether a different mAb or a cocktail of mAbs might offer better protection. One challenge to the development of such immunotherapeutics is that it appears difficult to elicit an effective antibody response in natural infection: many survivors have little to no IgG.[1] A second challenge is that of these antibodies that are elicited, whether by natural infection or by vaccination, the majority appear to preferentially react with sGP or cross-react between sGP and GP.[10,12,14,15] These antibodies may be absorbed by the much more abundant shed sGP and, thus, it may be difficult to achieve concentrations required for viral neutralization.

A murine IgG2a termed 13F6-1-2 has been identified which is specific for viral surface GP, does not cross-react to shed sGP, and is protective against challenge with the highly pathogenic Zaire subtype of the Ebola virus.[12] All mice (10/10) survive challenge with 300 times the lethal dose of Ebola virus when 100 μg of 13F6-1-2 is administered one day after challenge.[12] The epitope has previously been mapped to nine residues (EQHHRRTDN, amino acids 405–413) within the Ebola Zaire GP mucin-like domain.[12] These residues are contained within a heavily glycosylated mucin-like region unique to GP,[12] which has been linked to GP-induced cytotoxicity.[16]

Interestingly, 13F6-1-2 contains a rare $V\lambda_x$ light chain that is observed in only 0.5% of antibody sequences and is barely detectable in normal mouse serum.[17–19] $V\lambda_x$, first described in 1987,[17–19] is conserved among mice, humans, and other mammals,[20] and displays at least three features unique from $V\lambda1$ and $V\lambda2$. The amino acid sequence is only ~30–33% homologous to other known $V\lambda$ and/or $V\kappa$ light chains. The last codon of the $V\lambda_x$ gene is a TAA stop codon that must be disrupted by $J\lambda2$ to create a functional codon (Fig. 1). As a result of this V–J junction, four extra residues extend the complementarity-determining region (CDR) L3. Previous studies suggest that this unusual light chain confers antigen specificity to the antibodies that contain it.[21]

Characterization of the mode of recognition of GP by the protective 13F6-1-2 mAb and successful humanization of its sequence are necessary steps towards development of this antibody as an immunotherapeutic against the Ebola virus. Here we present the crystal structure of a complex between the Fab fragment of 13F6-1-2 and its GP epitope at 2.0 Å resolution. This work provides the first available structure of an antibody directed against the Ebola virus and illustrates unusual structural features of a $V\lambda_x$-containing antibody that shed light on its immunological relevance.

Results and Discussion

13F6-1-2 contains a rare $V\lambda_x$ light chain

Sequencing of 13F6-1-2 revealed the usage of a rare λ_x light-chain gene. The nucleotide sequence of the 13F6-1-2 $V\lambda_x$ light chain is 99.3% homologous to the previously reported BALB/c $V\lambda_x$ germ line (GenBank accession number M34597 or IGLV3 in IMGT nomenclature; Fig. 1a). Interestingly, there is only a single somatic mutation contained within all three CDRs. Indeed, $V\lambda_x$-bearing light chains in general have very little somatic mutation. Only two other $V\lambda_x$-bearing antibodies have been well described. One is termed F28C4 (GenBank accession number X76752), contains just two somatic mutations in the CDR L3 region (Fig. 1a), and is directed against myelin basic protein.[22] The second is termed MW1 (GenBank accession number M34598), contains no somatic mutations, and is directed against a poly-Gln sequence relevant for Huntington's disease.[23]

The 13F6-1-2 heavy chain belongs to the 7183 family, clone 19 (Fig. 1b), and shares 88% sequence identity with the V_H283 germ line. Of the 12 mismatches, 5 reside in the CDRs (Fig. 1b).

13F6-1-2 Fab structure

The crystallographic asymmetric unit contains one Fab 13F6-1-2:GP peptide complex. The polypeptides of the light and heavy chains are well defined by electron density except for five side chains (Glu H1, Gln L2, Arg L27, Gln L27A, and Asp L60), which have been truncated to alanine. Analysis of conformations by Ramachandran plot shows >99% of residues residing in favourable regions and no nonglycyl residues in disallowed regions. Note that in most Fab structures, residue 51 of the light chain exists in a γ turn in a rare region of the Ramachandran plot.[24] In the structure presented here, however, CDR L2 is noncanonical and residue 51 adopts a different, favoured conformation.

The $V\lambda_x$ light chain and heavy chain of 13F6-1-2 form the expected overall V-type, nine-stranded β-sandwich immunoglobulin fold (Fig. 2) and the light chain is, not surprisingly, similar to a recently determined $V\lambda_x$-bearing variable domain (MW1).[23] To our knowledge, this is the only other $V\lambda_x$ antibody structure for which a structure is available. While the overall $V\lambda_x$ fold of these structures is similar to the V-type immunoglobulin fold, there are a few unusual differences. In MW1 and 13F6-1-2, a one-residue deletion (typically, deletion of a proline or threonine) exists in the A–A′ strand, which results in a smaller kink and disruption of typical A–G strand hydrogen bonding (Fig. 2b).[23] In $V\lambda_x$, the C″ β-strand twists towards the outer D β-strand to form a pseudo-β-barrel, but the C″ β-strand of $V\lambda_x$ does not make any hydrogen bond interactions with strand D, as would occur in the immunoglobulin fold in T-cell receptors (TCRs).

The elbow angle between the variable and constant Fab domains in 13F6-1-2 is 149°. This is consistent with other $V\lambda$ light chains, which typically exhibit a bimodal distribution of elbow angles with values between 117° and 225°.[26] At the variable light chain/heavy chain (V_L/V_H) interface of 13F6-1-2, ~1025 Å^2 surface area is buried on V_L
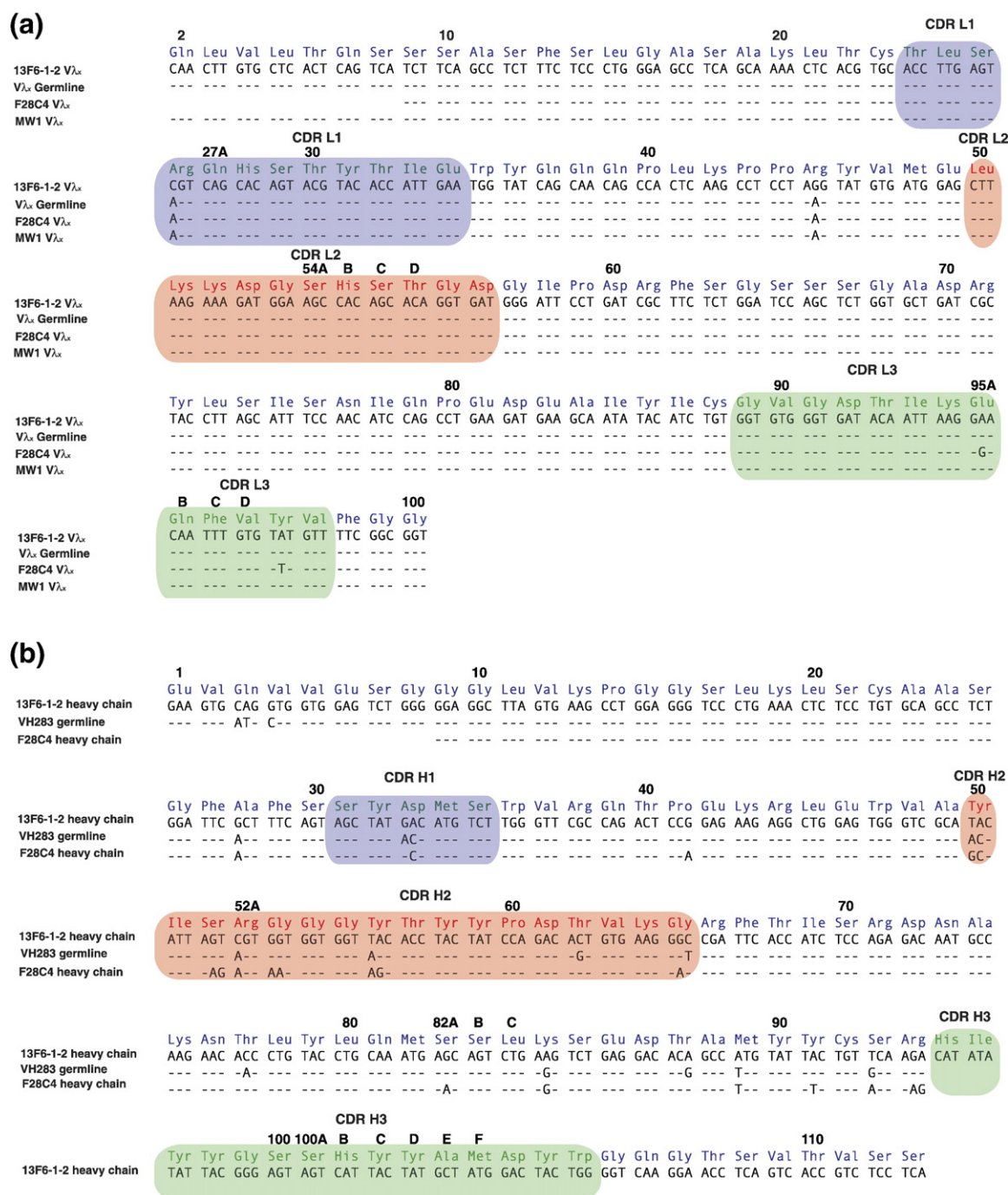
Fig. 1. Nucleotide and translated amino acid sequences for variable regions. (a) The light-chain variable region of 13F6-1-2 compared with the BALB/c Vλ$_x$ germ line (GenBank accession number M34597), and the Vλ$_x$ light chains F28C4 (GenBank accession number X76752) and MW1 (GenBank accession number M34598). 13F6-1-2 contains two mutations from the Vλ$_x$ germ line: a Ser to Arg mutation at residue 27 in CDR L1 and a Lys to Arg mutation in framework residue 45. (b) The heavy-chain variable region of 13F6-1-2 compared with the germ line V$_H$283 and F28C4. The amino acids are labeled according to the Kabat numbering scheme and hypervariable loops are highlighted in colour.

and ∼985 Å^2 on V$_H$. Interestingly, this is within the smaller range of light chain/heavy chain interfaces described for antibodies. The typical buried surface area ranges between 1068 and 1750 Å^2.[27,28] A small V$_H$/V$_L$ interface has been correlated with the ability to use domain rearrangements in the induced fit of the antibody to the antigen,[28] although it is unclear

whether an induced conformational change occurs in 13F6-1-2 upon peptide binding.

13F6-1-2 hypervariable loops

Complementarity-determining regions of antibodies are typically restricted to certain conforma-

(a)

(b)
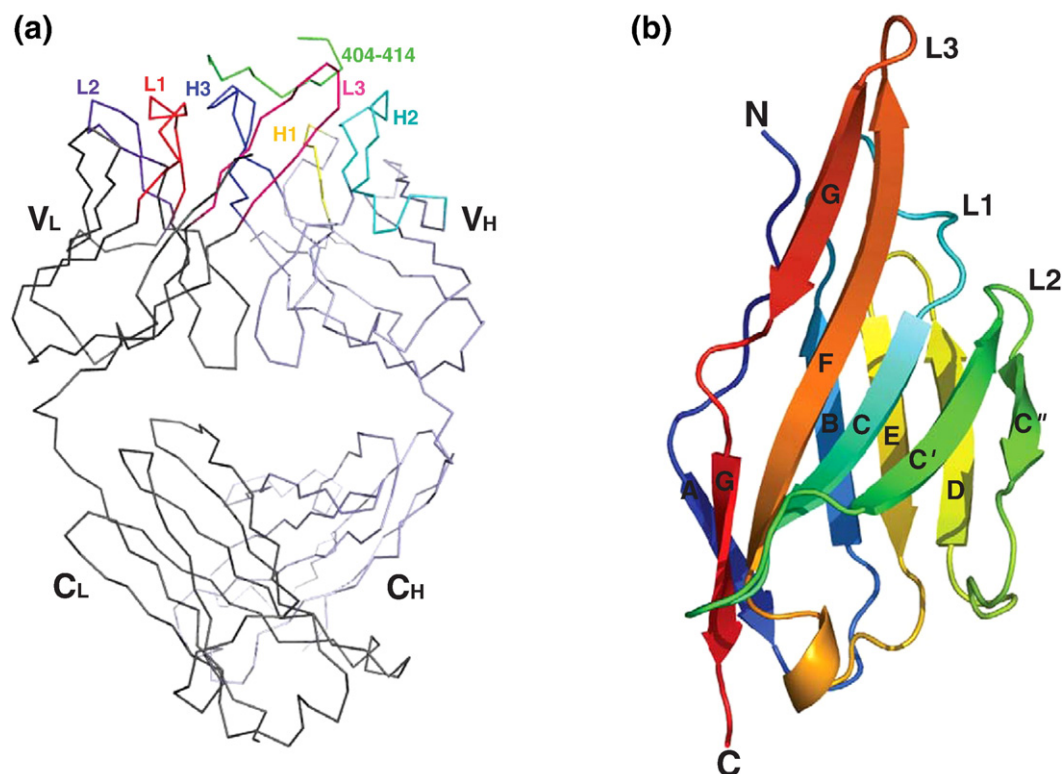
Fig. 2. Overall structure of 13F6-1-2. (a) C^{α} trace of the 13F6-1-2 Fab fragment complexed to the P404–P414 Ebola virus GP peptide. The structure is shown with bound GP peptide coloured in green, and the light and heavy chains in dark grey and light blue, respectively. CDRs L1, L2, L3, H1, H2, and H3 are coloured red, purple, pink, yellow, cyan, and blue, respectively. (b) Ribbon diagram of the 13F6-1-2 $V\lambda_x$ light-chain variable domain. β-Strands are labeled A, B, C, C′, C″, D, E, F, and G. This and subsequent figures were generated using MacPyMol.[25]

tions, depending on the length of insertion in the CDR. An analysis of 79 different hypervariable regions revealed that each can be assigned to at least one of 18 different canonical structures.[24] None of the CDRs of 13F6-1-2 are affected by crystal contacts. The heavy-chain CDRs H1 and H2 belong to canonical classes 1 and 3, respectively. CDR H3 contains 15 amino acids. Residues H92–H96 and H100e–H104 form an antiparallel β-sheet, and a type I β-turn exists between Tyr H97 and Ser H100 ($i+1$: $\varphi = -60.4°$, $\psi = -36.5°$; $i+2$: $\varphi = -55°$, $\psi = -28.5°$). By contrast, analysis of the light-chain $V\lambda_x$ CDR loops of 13F6-1-2 and MW1 reveals a new class of hypervariable loop structures.

CDR L1

The CDR Vλ L1 region normally falls into four different canonical conformations,[24,29–31] with the region typically containing 9 to 11 residues and a hydrophobic residue at center that packs into the antibody framework (Fig. 3a).[24] In canonical conformation 4, residues 26 to 30 form an irregular helix. Six canonical conformations have been identified for the CDR Vκ L1 region that typically contains between 6 and 13 residues[24] (Fig. 3b). In all six canonical conformations, residues 26 to 29 adopt an extended conformation and residues 29 to 32 adopt a short link or hairpin loop. Almost all human germ

line and expressed Vκ light chains have canonical structures 2, 3, 4, or 6.[32] The $V\lambda_x$ CDR L1 is 12 residues long and does not contain the standard helix or any other defined secondary-structure element (Fig. 3c). Interestingly, there is also no hydrophobic residue that packs into the framework in $V\lambda_x$, as the side chain of the equivalent residue (Ser29) points away from the framework.

CDR L2

The CDR L2 for standard Vλ and Vκ light chains always contains seven residues and occurs in only one known conformation, with a three-residue γ-hairpin loop linking the C′ and C″ β-strands (Fig. 3d).[24] In order to maintain the γ-hairpin loop, the residue at position 51 (usually a Val but also sometimes a Ser) typically lies in a rare conformation in the Ramachandran plot, with torsion angles of $\varphi = +67°$, $\psi = -40°$.[24] However, in $V\lambda_x$-bearing antibodies, four additional residues are inserted into the CDR L2 loop, for a total of 11 residues to form a type I β-turn (Fig. 3e). As a consequence, this insertion allows the formation of a longer β-sheet between β-strands C′ and C″ and allows the inner C″ β-strand to twist towards the outer β-strand D. The $V\lambda_x$ CDR L2 does not have a valine at position 51, but rather a lysine residue that resides in a favourable region of φ–ψ space and forms a hydrogen bond
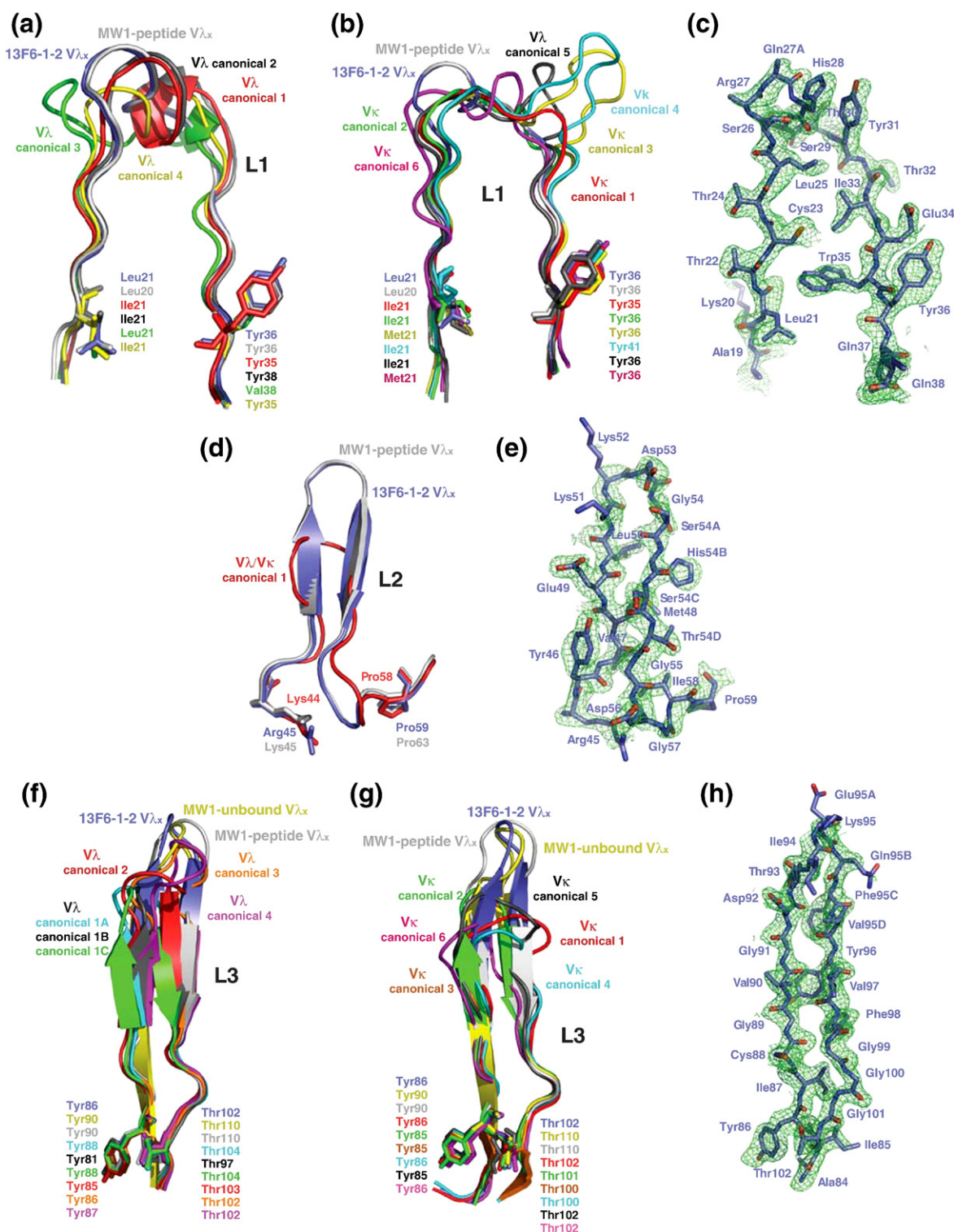
Fig. 3. Analysis of light-chain CDRs. Comparison of Fab 13F6-1-2 and (a) Vλ L1, (b) Vκ L1, (d) Vλ/Vκ L2, (f) Vλ L3, and (g) Vκ L3 CDR canonical conformations. The initial difference σ_A-weighted $F_o - F_c$ electron density map (green), contoured at 2σ, superimposed onto the refined (c) L1, (e) L2, and (h) L3 13F6-1-2 CDR structures. Example structures of CDR canonical conformations are taken from the following antibody structures (PDB accession codes in parentheses): CDR L1 Vλ canonical conformation 1 (2FB4), 2 (7FAB), 3 (1MFA), 4 (8FAB), MW1 peptide (2OTU); CDR L1 Vκ canonical conformation 1 (2FBJ), 2 (1VFA), 3 (1HIL), 4 (1FLR), 5 (1GGI), 6 (1FIG), MW1 peptide (2OTU); CDR L2 Vλ/κ canonical conformation 1 (2FB4), MW1 peptide (2OTU); CDR L3 Vλ canonical conformation 1A (1GIG), 1B (7FAB), 1C (1MFA), 2 (2FB4), 3 (1Q1J), 4 (2B0S), MW1 peptide (2OTU), MW1 unbound (2GSG); CDR L3 Vκ canonical conformation 1 (1HIL), 2 (2FBJ), 3 (1BQL), 4 (1DFB), 5 (1BAF), 6 (1EAP), MW1 peptide (2OTU), MW1 unbound (2GSG). CDR L1 and L2 of MW1 in the unbound state (PDB code 2GSG) are not shown in (a), (b), and (d) for figure clarity, as these CDRs are similar in conformation to those observed in the MW1 peptide-bound structure.

between its carbonyl oxygen and the amide nitrogen of Gly54.

CDR L3

The typical CDR L3 of a Vλ antibody adopts one of two main conformations (Fig. 3f).[24] Canonical conformation 1 is a six-residue hairpin, with two residues at the top of the loop forming the tight turn. The high-resolution structures available for canonical conformation 1 show three minor forms (A, B, and C), where the orientation of the peptide bond differs between residues 93 and 94. A hydrogen bond exists between the main-chain oxygen of residue 95 and the amide nitrogen of residue 92. Canonical conformation 2 consists of eight residues in the loop, with four residues forming the turn. More recently, two additional conformations (named as canonical conformations 3 and 4 in this article) have been identified for L3 in the structures of the λ light chain containing neutralizing anti-HIV-1 antibodies 447-52D and 2219,[33,34] which have 9- and 10-residue L3 loops, respectively. For Vκ antibodies, CDR L3 usually belongs to one of six canonical conformations (Fig. 3g). Canonical conformations 1, 3, 4, 5, and 6 do not form a β-sheet as typically seen in Vλ CDR L3, but instead form a loop (Fig. 3g), with conformation 1 being the most commonly observed.[24] Canonical conformation 2 forms a regular hairpin and residue 94 adopts a *cis*-proline conformation. By contrast, Vλ$_x$ light chains have a 10-residue CDR L3, which allows the loop to form a longer β-sheet. In 13F6-1-2, a type IV β-turn is found at the top of the loop (Fig. 3h).

A new class of CDR canonical conformations

It has been proposed that the Vλ$_x$ light chain of antibodies does not undergo significant affinity maturation *via* somatic mutation.[20] Indeed, although very few Vλ$_x$ light chains have been identified and sequenced, those that have been described do not vary significantly in sequence from germ line. For example, mAb 13F6-1-2 contains only one somatic mutation (which lies in CDR L1), MW1 contains zero mutations, and mAb F28C4 contains only two somatic mutations (which lie in CDR L3). In addition, the lengths of the hypervariable loops in the Vλ$_x$ light chains are conserved. The Vλ$_x$ germ line, mAb 13F6-1-2, MW1, and F28C4 all have CDRs L1, L2, and L3 of 12, 11, and 13 residues in length, respectively; no other antibody has been described with light-chain CDRs longer than those of Vλ$_x$-bearing light chains. It appears that the hypervariable loop conformations observed in the 13F6-1-2 and MW1 Vλ$_x$ structures may represent new L1, L2, and L3 canonical classes for Vλ$_x$ light chains.

Analysis of the CDRs of 13F6-1-2 and bound and unbound MW1 clearly reveals that the L1 and L2 regions of these Vλ$_x$ antibodies are quite similar to each other, fairly rigid, and not subject to antigen-induced conformational changes (Fig. 3). Similarly, although new noncanonical conformations have

been described for CDR L3,[33,34] fewer deviations have been noted for CDR L1 and CDR L2 of other Vλ and Vκ antibodies. In fact, for CDR L2, all non-Vλ$_x$ antibody structures determined to date adopt only one conformation[24] regardless of the type of light chain. Although CDRs L1 and L2 appear rigid, L3 is more flexible and the conformations of CDR L3 differ among 13F6-1-2 and the peptide-bound and unbound structures of MW1 (Fig. 3f and g). This is rather interesting as the 13F6-1-2 and MW1 CDR L3s are identical in sequence. Hence, a single CDR sequence can adopt multiple conformations.

13F6-1-2 Fab–peptide interactions

The 11-residue peptide used for cocrystallization (VEQHHRRTDND) corresponds to a region of the mucin-like domain of the Ebola Zaire GP. Residues P404–P414 (based on the numbering in Ebola Zaire GP) are unambiguously located in strong electron density (Fig. 4a). The average *B* value for the peptide residues is 26 Å^2, suggesting that these residues are well defined and ordered. Surface plasmon resonance experiments were performed on the intact Ebola virus and show that IgG 13F6-1-2 has $k_{on} = 7.00 \times 10^4$ M^{-1} s^{-1} and $k_{off} = 2.87 \times 10^{-3}$ s^{-1}, with a calculated affinity (K_d) of 41 nM (Fig. 5a). The synthetic VEQHHRRTDND peptide used in cocrystallization competes for binding with IgG 13F6-1-2 and the full-length GP [50% inhibitory concentration (IC$_{50}$) of ~3.5 μM] (Fig. 5c). The competition is not as strong as expected, suggesting that additional contacts with the native GP protein may be made by 13F6-1-2, or that the conformation of the linear epitope may be stabilized in the context of the intact GP molecule.

Antibody–peptide interactions

Nine of the 11 peptide residues (residues P404–P412) are in contact with the antibody paratope. Asn P413 and Asp P414 turn away from the antibody and form two crystal contact hydrogen bonds to symmetry-related Fab residues Asn L164 and Leu H170, respectively. The epitope mapping results (data not shown) agree with our structural model and confirm that the epitope residues 413 and 414 are not important for binding 13F6-1-2.

In total, five hydrogen bonds are formed between the Vλ$_x$ light chain and the GP peptide (Fig. 4b and c). The amino group of Val P404 and the amide nitrogen of His P407 make main-chain hydrogen bonds to the carbonyl oxygen of Ala L27 and the O^{δ1} of Asp L92, respectively. The side chain of Gln P406 is anchored by three Vλ$_x$ main-chain hydrogen bonds to the main-chain nitrogen and oxygen of Thr L32 and the carbonyl oxygen of Gly L91.
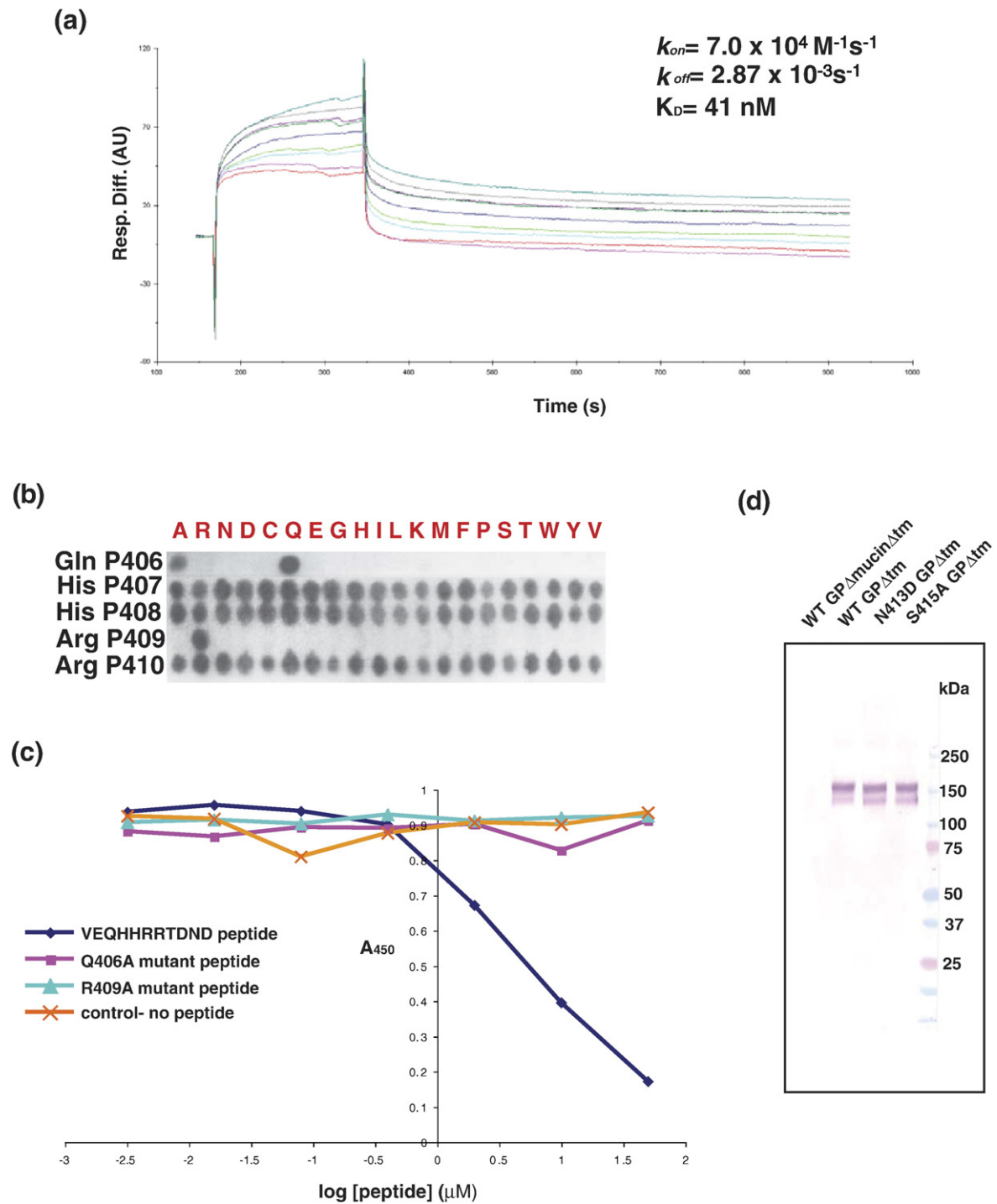
Fourteen hydrogen bonds are formed between the heavy chain and the GP epitope peptide (Fig. 4b and c). The carbonyl oxygen of His P407 makes a hydrogen bond with the Tyr H100D O^{η}, and the amide nitrogen of Arg P409 forms a 3.0-Å hydrogen-bond interaction with the carbonyl oxygen of His
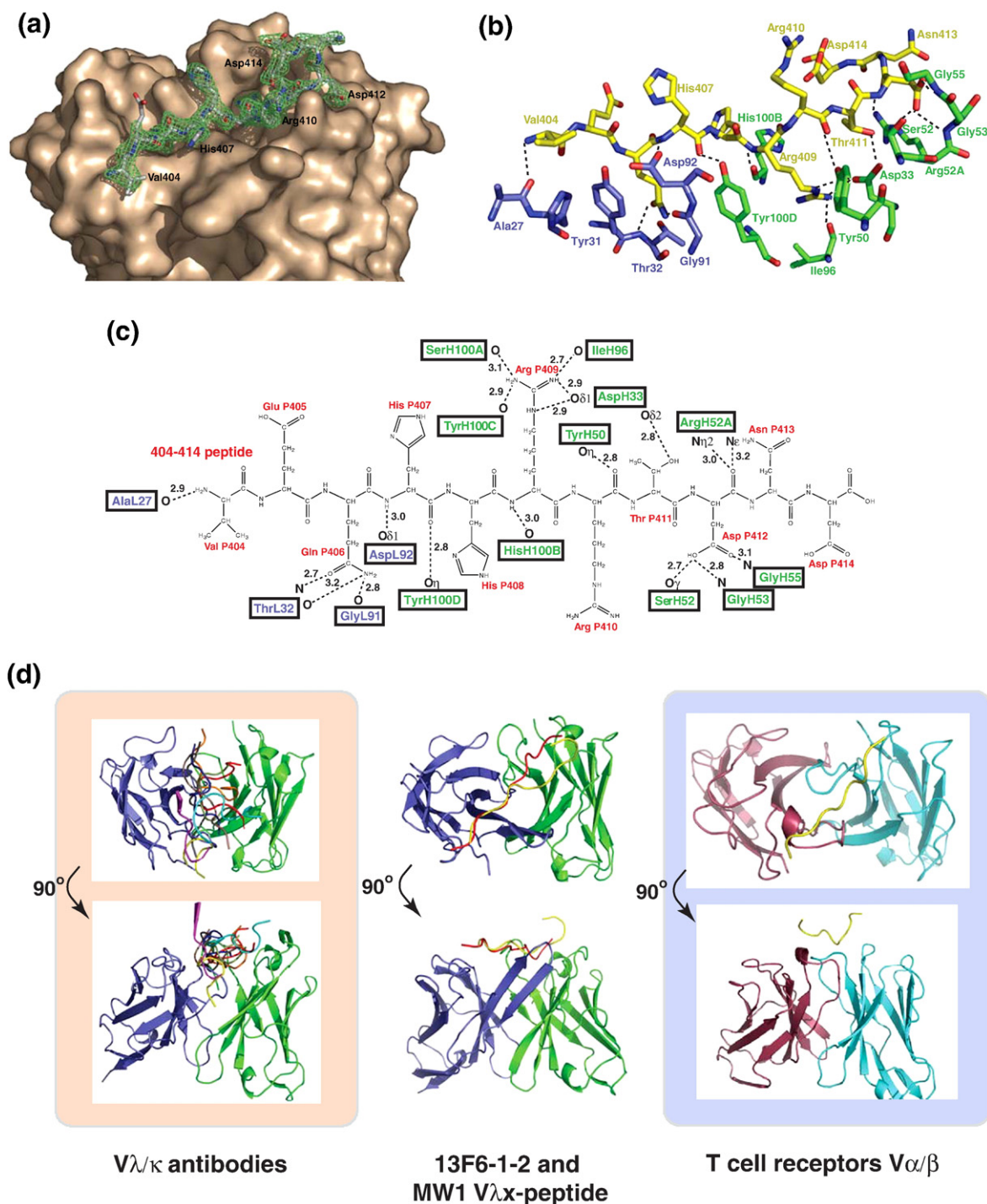
Fig. 4. Antigen-binding site. (a) Electron density for the P404–P414 GP peptide bound to 13F6-1-2. The initial difference σ_A-weighted $F_o - F_c$ electron density map (green), contoured at 3σ, superimposed onto the refined P404–P414 peptide and the molecular surface of 13F6-1-2. (b) Stick representation of the antigen-binding site in which peptide residues are coloured yellow, light-chain residues are blue, and heavy-chain residues are green. (c) 2-D schematic of the interactions between the peptide and Fab 13F6-1-2. Peptide residues are illustrated in black and labeled in red. (d) Comparison of general peptide-binding orientations in Vλ/Vκ antibodies and Vα/β TCRs that bind peptides in a diagonal orientation. For all figures, the light and heavy chain and the TCR Vα and Vβ chains are coloured purple, green, red, and cyan, respectively. The light and heavy chains of all antibodies or α/β chains were superimposed. However, for clarity, only the peptide is shown (PDB code 1CU4, red; 1TJG, brown; 1F58, blue; 1ACY, green; 1NAK, yellow; 1SM3, magenta; 1GGI, cyan; 1CFN, orange; and 1CE1, black). In the middle panel, the poly-Gln peptide bound to MW1 (PDB code 2OTU) and GP peptide bound to 13F6-1-2 are shown in red and yellow, respectively.

(a)

k_{on}= 7.0 x 10^4 M^{-1}s^{-1}
k_{off}= 2.87 x 10^{-3}s^{-1}
K_D= 41 nM

(b)

A R N D C Q E G H I L K M F P S T W Y V

Gln P406
His P407
His P408
Arg P409
Arg P410

(d)

WT GPΔmucinΔtm
WT GPΔtm
N413D GPΔtm
S415A GPΔtm

(c)

- VEQHHRRTDND peptide
- Q406A mutant peptide
- R409A mutant peptide
- control- no peptide

Fig. 5. Binding analysis of 13F6-1-2 to the GP peptide epitope. (a) 13F6-1-2 kinetic surface plasmon binding response to Ebola virus (Zaire-1995 strain). Five concentrations were injected at 30 μL/min and the k_{on} and k_{off} rates were calculated based on 1:1 Langmuir binding. (b) SPOTs membrane-binding analysis of the 13F6-1-2 epitope. Peptides containing complete 20 amino acid replacement mutations to 13F6-1-2 peptide epitope residues Gln P406, His P407, His P408, Arg P409, and Arg P410 were synthesized onto a cellulose membrane. The membrane was incubated with IgG 13F6-1-2 and bound 13F6-1-2 was detected with an anti-mouse β-galactosidase-conjugated secondary antibody. (c) Competition ELISA of 13F6-1-2 and mutant epitope peptides. Microplates were coated with GP (transmembrane deletion) and incubated with IgG 13F6-1-2 and either the peptide epitope mimic or a mutant (Gln406Ala or Arg409Ala) epitope peptide. Bound 13F6-1-2 was detected by incubating with horse anti-mouse horseradish peroxidase secondary antibody. (d) Nondenaturing Western blot analysis of Asn413Asp and Ser415Ala GP mutants. WT GPΔmucinΔtm (wild-type GP with deletions of the mucin and transmembrane domains), WT GPΔtm, Asn413Asp GPΔtm, and Ser415Ala GPΔtm were probed for binding with IgG 13F6-1-2 antibody. WT GPΔmucinΔtm and WT GPΔtm were used as the negative and positive controls, respectively.

Table 1. Comparison of peptide–antibody complexes

PDB code	Resolution (Å)	Peptide length/residues bound	Buried SA V_H/V_L–peptide (Å²)	Buried SA V_L–peptide (Å²)	Buried SA V_H–peptide (Å²)	Buried SA L1–peptide (Å²)	Buried SA L2–peptide (Å²)	Buried SA L3–peptide (Å²)	Buried SA H1–peptide (Å²)	Buried SA H2–peptide (Å²)	Buried SA H3–peptide (Å²)	Sc index
2QHR (13F6-1-2 $V\lambda_x$)	2.0	11/9	1613	648	1176	348	0	377	133	533	706	0.78
2OTU (MW1-peptide $V\lambda_x$)	1.68	12/11	1687	885	855	553	0	358	467	90	430	0.76
1CU4	2.9	10/9	1428	596	919	345	55	259	427	342	264	0.75
1TJG	2.0	7/6	1004	464	673	0	0	469	128	300	392	0.78
1F58	2.0	10/10	1408	725	852	438	0	364	185	205	511	0.79
1ACY	3.0	10/7	1037	498	633	251	0	333	141	222	394	0.81
1NAK	2.57	10/9	1074	553	623	225	171	230	267	0	410	0.78
1SM3	1.95	9/9	1031	444	757	160	106	235	150	95	64	0.75
1GGI	2.8	9/7	1094	560	739	126	116	292	170	59	121	0.79
1CFN	2.65	10/10	1007	501	602	166	103	251	336	57	228	0.56
1CE1	1.9	7/7	873	491	573	98	38	414	164	168	323	0.80
Average	2.3	9.5/8.5	1205	579	764	246	54	326	233	188	349	0.76

SA, surface area; Sc, surface complementarity.

H100B. The guanidinyl group of Arg P409 is strongly anchored by five hydrogen bonds to the main-chain oxygen atoms of Ile H96, Ser H100A, and Tyr H100C and the side chain $O^{\delta 1}$ of Asp33. The interaction of Asp H33 and the positively charged guanidinyl group of Arg P409 likely form a stabilizing salt bridge. Arg P410 only makes a main-chain carbonyl hydrogen bond with the O^{η} of Tyr H50. The Thr P411 O^{γ} makes a tight hydrogen bond (2.8 Å) with the Asp H33 $O^{\delta 1}$. Arg H52A $N^{\eta 2}$ and N^{ε} make weaker hydrogen bonds (3.0 and 3.2 Å, respectively) with the main-chain oxygen of Asp P412. The side chain of Asp P412 is stabilized by three strong hydrogen bonds with Ser H52 O^{γ} and the main-chain amide nitrogen atoms from Gly H53 and Gly H55.

Peptide-binding mode

Peptide residues VEQHHRRTD (residues P404–P412) adopt an extended linear conformation that lies diagonally across the light and heavy chains in a groove that is ~28 Å long and 10 Å wide (Fig. 4a). In antipeptide antibody structures, the peptide typically binds at the interface between the light and heavy chains (Fig. 4d). However, the peptide-binding mode seen in 13F6-1-2 is rather unusual in that the peptide epitope lies diagonally across the light and heavy chains rather than at the light chain/heavy chain interface (Fig. 4d). This orientation is reminiscent of some TCRs, in which the bound peptide binds diagonally across both the Vα and Vβ chains[35] (Fig. 4d). To date, there are no other non-$V\lambda_x$ antibody complexes known to exhibit such an extended diagonal binding nature. In addition, peptides typically form somewhat more contacts with the heavy chain than with the light chain. 13F6-1-2 interactions are skewed more towards the heavy chain, which forms 73% of the buried surface area. By contrast, in $V\lambda_x$ MW1, the V_H and V_L domain interactions are shared about equally (Table 1).

In 13F6-1-2, the GP peptide makes significant contacts with CDRs L1, L3, H1, H2, and H3, and ~1600 Å² of antibody surface area is buried by peptide binding (Table 1). No contacts are formed with CDR L2 due to the diagonal orientation of the peptide. In the light chain, the peptide-binding groove is shallow and open, while in the heavy chain, the groove is more complementary to the peptide shape and contains a deep pocket to accommodate the side chain of Arg P409.

Insight into the mucin-like domain

The mucin-like domain of Ebola virus GP is heavily glycosylated with both N- and O-linked oligosaccharides. Residues encompassing the 13F6-1-2 epitope contain two potential glycosylation sites: a possible O-linked site at Thr P411 and a possible N-linked site at Asn P413. However, the NetOGlyc/NetNGlyc servers† do not predict a high glycosyla-

---

† http://www.cbs.dtu.dk/services

tion potential for either of these sites (R. Gupta, E. Jung, and S. Bruna, unpublished results). In the crystal structure, the Thr P411 side chain is directed into a complementary-shaped site on the antibody paratope, and the restricted cavity of the antibody would prevent an O-glycosylated Thr P411 from properly binding 13F6-1-2. Asn P413 lies just outside of the antigen-binding site and its side chain is pointed out into the solvent channel, so 13F6-1-2 could theoretically accommodate an oligosaccharide at this position. However, GP containing either of two point mutations that remove the N-X-S glycosylation motif (Asn413Asp and Ser415Ala) retains 13F6-1-2 binding (Fig. 5d), suggesting that these residues or a glycan at this site is not involved in 13F6-1-2 binding. The crystal structure of 13F6-1-2 in complex with this extended, nonglycosylated region of the mucin-like domain suggests that there may be other similarly nonglycosylated stretches of extended structure on the surface of Ebola GP accessible to neutralizing antibodies.

Role of the Vλ$_x$ light and heavy chains in antigen binding

Most antibodies utilize residues in both the heavy and light chains for antigen binding and recognition. Our structural and functional data show that the Vλ$_x$-bearing 13F6-1-2 likely exploits both the heavy and light chains for recognition, but primarily the heavy chain for tight binding.

Only four peptide side chains interact with antibody residues: Gln P406 contacts the light chain, while Arg P409, Thr P411, and Asp P412 contact the heavy chain. Of these, Gln P406 and Arg P409 form the most extensive interactions with antibody (Fig. 4b and c), and SPOTs membrane analysis and competition ELISAs of peptide mutants reveal that these two residues are important for binding. A complete amino acid replacement series mutagenesis of the 13F6-1-2 epitope by SPOTs analysis shows that positions P407, P408, and P410 can tolerate substitutions to any amino acid, but Arg P409 needs to be strictly conserved. Position P406 can only tolerate an alanine substitution (Fig. 5b) by SPOTs binding; although a peptide containing a Gln406Ala mutation cannot compete with wild-type GP for 13F6-1-2 binding (Fig. 5c).

Gln P406, the third residue in the epitope, makes three contacts with the light chain. Arg P409, the sixth residue in the epitope, makes five contacts with the heavy chain (Fig. 4c). Interestingly, in another Vλ$_x$-bearing antibody, F28C4, NMR experiments have determined that the third and sixth positions of the epitope (Gln 3 and Pro 6) are also important for recognition.[22] Similarly, in the MW1–peptide complex, Gln 4 is found in the third position of the epitope and makes substantial contact with the antibody. Hence, all Vλ$_x$-bearing antibodies studied require a glutamine residue at the third position of the epitope for recognition. This is not surprising, as all known Vλ$_x$-bearing antibodies contain very few somatic mutations and primarily utilize germ-line-encoded residues to mediate antigen binding (Fig. 1), and binding of this glutamine in particular.

Although the light chain plays a role in recognition, it is not thought to play a major role in tight binding. In 13F6-1-2, the heavy chain forms 73% of the buried surface area (Table 1). The heavy chain also forms one electrostatic interaction and 13 hydrogen bonds to binding, while the light chain forms only five hydrogen bonds. The electrostatic salt bridge between heavy-chain Asp H33 and Arg P409 likely dictates tight binding, as typical hydrogen bonds only provide 0.5–1.5 kcal/mol of binding energy.[36] A simple calculation using Coulomb's law, by approximating a positive and negative point charge moving from infinity or an unbound state to 2.9 Å, shows that this salt bridge may contribute a binding energy of up to 28.6 kcal/mol (dielectric constant = 4). This binding energy is more than sufficient to account for the observed 41 nanomolar affinity of 13F6-1-2 for GP.

Ebola virus vaccine development and prophylactic treatment

Although development of a vaccine against the Ebola virus is a high priority, prophylactic vaccination against a rare pathogen may not be economically feasible for much of the population. Development of immunotherapeutics would provide an immediate, valuable treatment option in the event of viral exposure or release. However, there are several challenges to the development of efficacious antibody-based therapies for Ebola virus GP. Many survivors of Ebola virus infection display no or low titers of neutralizing antibody,[37–40] perhaps because the disease course outcompetes the speed with which the immune system can generate virus-specific IgG. In addition, the virion-attached GP is heavily glycosylated and much of its surface may be masked from immune surveillance. Plus, those antibodies that are in survivor sera appear to preferentially recognize the sGP rather than the virion-attached GP,[15] even though these two proteins share the first 295 amino acids. This suggests that certain antibody epitopes may be better exposed on sGP, or that sGP competes for antibody binding as it outnumbers the virion-attached GP by approximately fivefold. Development of efficacious antibodies specific for virion-attached GP would allow more efficient immunotherapeutic targeting of virions and infected cells.

The 13F6-1-2 epitope may be a good target for vaccine and immunotherapeutic design, as it is immunodominant in a murine model and provides protection against viral challenge.[12] In addition, the peptide epitope belonging to residues P404–P412 is bound in an extended conformation and does not adopt any secondary structure (i.e., β-turns, helices, β-sheets) or posttranslational modifications that would be difficult to achieve in synthetic or recombinant systems.

When murine antibodies can be successfully humanized, they can provide clinical benefit.[41] Fortunately, BLAST searches of 13F6-1-2 reveal that the human Vλ subgroup VIII light chain shares significant framework sequence identity with the rare Vλ$_x$ light chain (~80%), with only 13 amino acid differences (Fig. 6a). In addition, the unusual lengths of the CDR L1 and L2 regions are similar between 13F6-1-2 and the human Vλ (VIII) germ line. Hence, human Vλ (VIII) could be used as a template for humanization of 13F6-1-2. Our 13F6-1-2 crystal structure will provide an excellent model to understand which interactions between the framework and the CDRs must be conserved to maintain antigen-binding affinity. From the 13 framework residues that differ between human Vλ (VIII) and 13F6-1-2, only three of these residues appear to stabilize the CDRs. Tyr L36, Asp L70, and Ser H105 hydrogen-bond to key residues in the L3, L1, and L2 CDRs, respectively (Fig. 6b) and may need to be maintained in any humanized molecule in order to conserve the stabilizing framework–CDR interactions necessary for peptide binding. We are currently evaluating the humanization potential of 13F6-1-2 as a postexposure therapeutic against the Ebola virus.

Conclusions

In summary, we have determined the sequence and the structure of the anti-Ebola virus Fab 13F6-1-2 in complex with its GP epitope to 2.0 Å resolution. 13F6-1-2 utilizes a rare Vλ$_x$ light chain, which displays several unusual structural features. In comparison with one other available structure of a Vλ$_x$-bearing light chain, we propose a separate class of canonical hypervariable loops for Vλ$_x$ antibodies, distinct in structure from those of other Vλ and Vκ light chains. The Ebola GP peptide epitope is bound in a diagonal orientation, in which the first four peptide residues are bound by the light chain and the last five are anchored by the heavy chain. Light-chain contacts with the peptide are mediated only through germ-line-encoded residues, yet are critical for antigen recognition. The crystal structure of the 13F6-1-2–GP peptide complex thus adds to our knowledge of antibody–antigen recognition and provides a template for development of vaccines against the Ebola virus and for humanization of the mAb as a postexposure therapeutic.
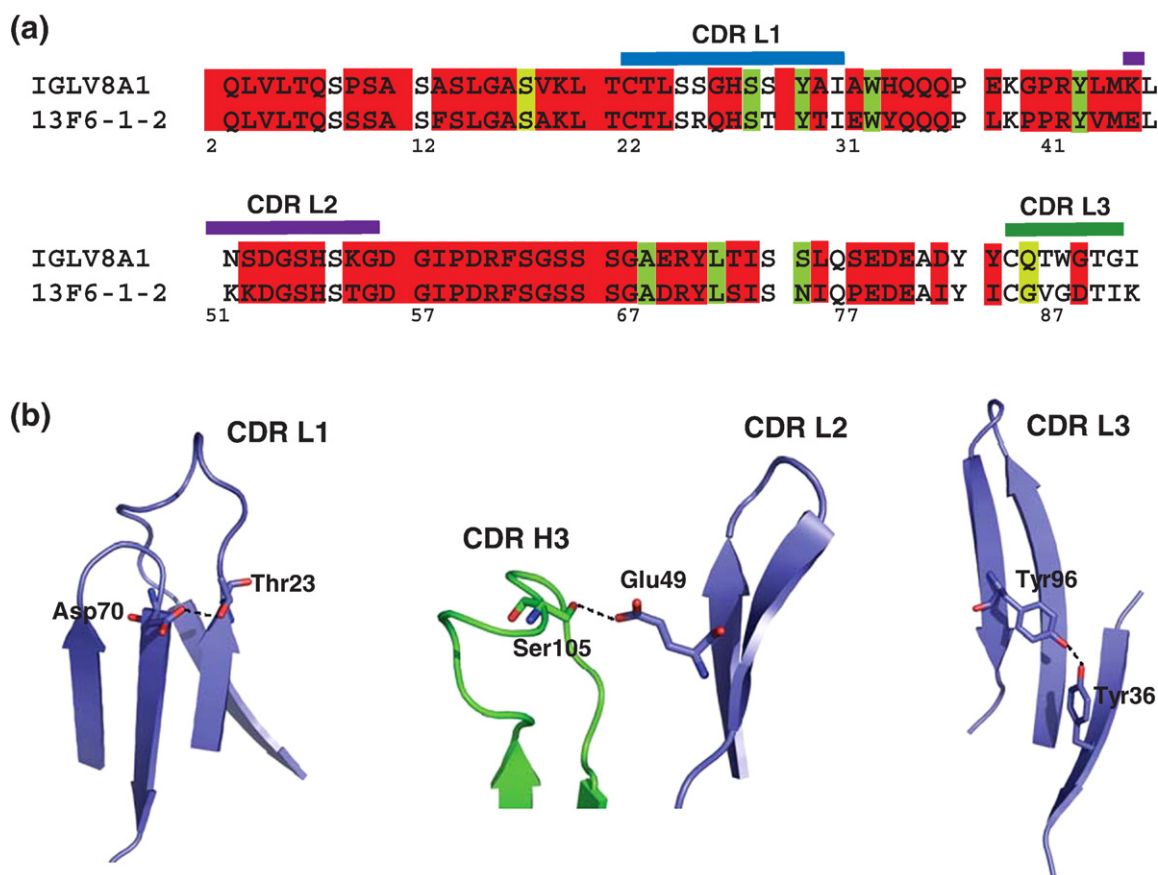
Fig. 6. Similarity of 13F6-1-2 Vλ$_x$ and human germ line Vλ subtype VIII light chains. (a) Sequence alignment of the 13F6-1-2 Vλ$_x$ light chain with human germ line Vλ subtype VIII light chain (GenBank accession number L29806). (b) Three framework residues of 13F6-1-2 interact with the CDRs and may need to be maintained in humanization. Asp L70 hydrogen bonds to Thr L23 in CDR L1, Ser H105 hydrogen bonds to Glu L49 of CDR L2, and Tyr L36 interacts with Tyr L96 from CDR L3.

Materials and Methods

Fab 13F6-1-2 production, purification, and sequencing

BALB/c mice were vaccinated and boosted with packaged Venezuelan equine encephalitis virus replicons encoding the GP from the Mayinga isolate of Ebola virus Zaire 1976, as previously described.[12] Spleen cells were harvested 3 days after the final injection and fused to P3X63Ag8.653 myeloma cells. Hybridoma screening was performed by ELISA and large-scale production of the antibody was carried out in Integra Celline flasks in serum-free medium. mAbs were purified from the supernatants on Protein G affinity columns and dialyzed in phosphate-buffered saline (PBS). The 13F6-1-2 Fab fragments were prepared by 1% v/v papain digestion at 37 °C for 1 h. Fab, Fc fragments, and undigested IgG2a were separated by Protein A chromatography. Fab collected in the Protein A flow-through was further purified by size exclusion on a Superdex 200 10/300 GL column equilibrated with 10 mM Tris–HCl (pH 7.5) and 150 mM NaCl. Sequencing of the variable regions was carried out as described in U.S. Patent 6,875,433.

Fab 13F6-1-2 peptide structure determination

Crystallization

An 11-residue peptide (VEQHHRRTDND) containing residues P404–P414 of the variable mucin-like C-terminus of GP1 was synthesized by the Center for Protein Sciences at The Scripps Research Institute. Fab 13F6-1-2 was concentrated to 15 mg/mL and preincubated with a fivefold molar excess of peptide (>95% purity) on ice for 30 min prior to crystallization by hanging-drop vapour diffusion at 22 °C. Crystals sufficient for data collection appeared directly from the sparse matrix screens overnight from Emerald Biosystems Wizard III condition 32 [16% (w/v) PEG 8000, 0.04 M potassium phosphate, and 20% (v/v) glycerol].

Data collection

In preparation for data collection at 100 K, crystals of the Fab 13F6-1-2–GP peptide complex were gently soaked 1 min in 20% (w/v) PEG 8000, 0.04 M potassium phosphate, and 25% (v/v) glycerol prior to flash cooling in liquid nitrogen. Data were measured at Beamline 8.2.2, Advanced Light Source (Lawrence Berkeley National Laboratory, Berkeley, CA) using an ADSC Q315 CCD detector. The data were indexed, integrated, and scaled with d*TREK (version 9.4).[42] Data collection statistics are presented in Table 2.

Structure determination and refinement

The structure of Fab 13F6-1-2–peptide complex was determined by molecular replacement using a murine IgG2a Fab fragment [Protein Data Bank (PDB) code 1YEC] as the initial search model. The program CNS SOLVE (version 1.1)[43,44] was used during all stages of structure determination and refinement. Data between 15 and 4 Å resolution were included in the cross rotation and translation functions in which a clear, unique solution was identified. Coordinates corresponding to this molecular replacement solution were subsequently subjected to a round of rigid body and torsion angle simulated annealing using all data, with no σ cutoffs. The R_{cryst}

Table 2. Data collection and refinement statistics

Diffraction statistics	
Space group	$P2_12_12_1$
	$a=68.2$ Å, $b=70.3$ Å,
	$c=142.1$ Å, $\alpha=\beta=\gamma=90°$
No. of observed reflections	188,364
No. of unique reflections	46,873
Resolution range (Å)	46.3–2.0
R_{sym} (%)[a]	8.4 (52.3)[b]
Redundancy	4.0 (3.5)[b]
Completeness (%)	99.7 (99.7)
Average $I/\sigma(I)$	6.8 (1.7)
Refinement statistics	
No. of total atoms	3659
No. of peptide atoms	98
No. of water molecules	233
Resolution range (Å)	46.3–2.0
R_{cryst} (%)[c]	20.3
R_{free} (%)[c]	24.5
Overall *B*-factor (Å^2)	24.3
Chain H	20.9
Chain L	27.0
Peptide	26.0
Water	29.0
rmsd	
Bonds (Å)	0.015
Angles (°)	1.3
Dihedrals (°)	11.2
Impropers (°)	1.1
Cross-validated coordinate error	
Luzatti (Å)	0.28

  a $R_{sym}=\sum\sum|I(k)-<I>|/\sum I(k)$, where $I(k)$ and $<I>$ represent the diffraction intensity values of the individual measurements and the corresponding mean values, respectively. The summation is over all unique measurements.
  b Values given in parentheses refer to reflections in the outer resolution shell: 2.07–2.00 Å.
  c $R_{cryst}=(\sum_{hkl}||F_o|-k|F_c||)/(\sum_{hkl}|F_o|)$, where F_o and F_c are the observed and calculated structure factors, respectively. For R_{free}, the sum is extended over a subset of reflections (5%) excluded from all stages of refinement.

and R_{free} prior to the first round of manual rebuilding were 38.7% and 41.6%, respectively. The interactive computer graphics program Xfit[45] was used to rebuild the initial model to the correct Fab 13F6-1-2 sequence and alternated with rounds of torsion angle simulated annealing starting at 5000 K[43,46] using all data with no σ cutoffs and bulk solvent correction. The progress of the refinement was monitored by reductions in R_{cryst} and R_{free}. Difference Fourier maps calculated after changing the model to the correct sequence of Fab 13F6-1-2 revealed strong unambiguous positive electron density corresponding to the P404–P414 peptide. Water molecules were included into the model during the later rounds of refinement based on the presence of positive 3σ peaks in the σ_A-weighted F_o-F_c difference electron density maps and at least one hydrogen bond to a protein, peptide, or solvent atom. After the addition of water molecules and the peptide, alternating rounds of crystallographic conjugate-gradient minimization refinement and model rebuilding were performed. The final model was refined in Phenix[47–49] with TLS refinement.[50] Refinement statistics are reported in Table 2.

Structural superimpositions were performed using the FATCAT‡ pairwise alignment server.[51] Shape complementarity index and buried surface area were calculated

‡ http://fatcat.burnham.org/fatcat/

using the program Sc[52] in the CCP4 suite and CNS-SOLVE,[44] respectively.

Analysis of peptide and mutant peptide binding

Surface plasmon resonance binding analysis

The binding analysis was performed using a CM-5 sensor chip on a BIAcore3000 at room temperature at the USAMRIID Biosafety Level 4 laboratory (Frederick, MD). A total of 6500 response units of sucrose-gradient-purified Ebola virus (Zaire 1995 strain) were immobilized using amide coupling chemistry to flow cell 1. Bovine serum albumin (BSA) was immobilized by amide coupling in flow cell 2 and both flow cells were washed with NaOH to stabilize the surface. IgG 13F6-1-2 was diluted to 0, 10, 25, 50, 100, and 500 nM. Each concentration was injected at 30 μL/min twice over flow cell 1 followed by flow cell 2 as a reference and data from flow cell 2 was subtracted out. The surface was regenerated with 10 mM glycine at pH 2.0. The final response unit was monitored for any buildup or degradation of the surface. A mass transfer test was used by injecting 100 nM 13F6-1-2 at three different flow rates (5, 15, and 75 μL/min). The k_{on} and k_{off} values were calculated based on a 1:1 Langmuir binding curve.

SPOTs membrane peptide array

Peptides containing complete 20 amino acid replacement mutations to 13F6-1-2 epitope residues Gln P406, His P407, His P408, Arg P409, and Arg P410 (peptide sequences: QVExHHRRTDNDST, QVEQxHRRTDNDST, QVEQHxRRTDNDST, QVEQHHxRTDNDST, and QVEQHHRxTDNDST) were custom synthesized onto a cellulose membrane by Sigma-Genosys and used according to the manufacturer's instruction. The membrane-immobilized peptides were rehydrated with 1× Tris-buffered saline (TBS, pH 8.0) and incubated at room temperature overnight with T-TBS blocking buffer [TBS, 0.05% (v/v) Tween 20, 5% (w/v) sucrose, and 10% (v/v) Genosys concentrated blocking buffer]. The membranes were washed three times with T-TBS before incubation with 20 mL of IgG 13F6-1-2 at a concentration of 5 μg/mL for 3 h at room temperature. Unbound antibody was removed by three washes of T-TBS and bound 13F6-1-2 was detected using an anti-mouse β-galactosidase-conjugated secondary antibody. After 2 h incubation at room temperature, the membranes were washed twice with T-TBS and twice with PBS. The bound antibody was visualized using a signal development solution (potassium ferricyanide, 5-bromo-4-chloro-3-indolyl-β-D-galactopyranoside, magnesium chloride in PBS).

Competition ELISAs

Peptides containing alanine point mutations were synthesized by AnaSpec (peptide sequences: VEAHHRRTDND and VEQHHARTDND). Corning Costar 96-well microplates were immobilized with recombinant, soluble full-length Ebola virus GPΔtm (lacking the transmembrane domain) (0.05 mL, 10 μg/mL) overnight at 4 °C. Microplates were blocked with 0.1 mL of 3% (w/v) BSA for 1 h at 22 °C. Twenty-five microliters each of IgG 13F6-1-2 antibody [1.5 μg/mL final concentration in PBS with 1% (w/v) BSA] and peptide epitope mimic or mutant peptide epitope (0 to 50 μM final concentration in PBS with 1% (w/v) BSA was added to the microplates and incubated for 2 h at 22 °C. After the plates were washed

with PBS with 0.05% (w/v) Tween 20, bound IgG 13F6-1-2 was detected by incubation with horse anti-mouse horse-radish-peroxidase-conjugated secondary antibody (0.05 mL, 1:2500 dilution) for 1 h at 22 °C. Each well was then washed 10 times with PBS containing 0.05% (w/v) Tween 20. The product was developed using the Pierce TMB substrate kit according to the manufacturer's protocol. Colour development was read immediately in a Molecular Devices VersaMax microplate reader at 450 nm.

Analysis of the Asn413 glycan sequon

Asn413Asp and Ser415Ala GP mutations were generated using the QuikChange II site-directed mutagenesis kit (Stratagene), according to the manufacturer's protocol. Wild-type (WT) GPΔtm, WT GPΔmucinΔtm, Asn413Asp GPΔtm, and Ser415Ala GPΔtm DNA were transiently transfected into HEK293T cells using FuGene6 in six-well culture plates. Supernatants were harvested 4 days posttransfection. Twelve microliters of supernatant was loaded in each lane and analyzed by nondenaturing Western blot using mouse 13F6-1-2 monoclonal primary antibody (2 μg/mL), followed by goat anti-mouse IgG peroxidase-conjugated secondary antibody (1:1000 dilution). The signal was visualized using Sigma FAST BCIP/NBT.

Nucleotide and protein accession codes

Nucleotide and protein sequences for IgG2a 13F6-1-2 light and heavy chains were published in U.S. Patent 6,875,433 and are accessible through the U.S. Patent and Trademark Office Web site§.

Protein Data Bank accession code

The coordinates and structure factors for the Fab 13F6-1-2–peptide complex have been deposited in the Research Collaboratory for Structural Bioinformatics Protein Bank‖ with PDB accession code 2QHR.[53]

Acknowledgements

§ http://www.uspto.gov
‖ http://www.rcsb.org/pdb

References

1. Peters, C. J., Sanchez, A., Rollin, P. E., Ksiazek, T. G. & Murphy, G. A. (1996). Filoviridae: Marburg and Ebola viruses. In *Fields Virology* (Fields, B. N., Knipe, D. M. & Howley, P. M., eds), 3rd edit., vol. 1, pp. 1161–1176, Lippincott-Raven Press, Inc., Philadelphia, PA.

2. World Health Organization. (2004). Ebola Haemorrhagic Fever, World Health Organization, Geneva, Switzerland.

3. Johnson, K. M., Lange, J. V., Webb, P. A. & Murphy, F. A. (1977). Isolation and characterization of a new virus causing acute hemorrhagic fever in Zaire. *Lancet*, **1**, 569–571.

4. Khan, A. S., Tshioko, F. K., Heymann, D. L., Le Guenno, B., Nabeth, P., Kerstiens, B. *et al.* (1999). The reemergence of Ebola hemorrhagic fever, Democratic Republic of the Congo, 1995. Commission de Lutte contre les Epidemies a Kikwit. *J. Infect. Dis.* **179**, S76–S86.

5. Sanchez, A., Yang, Z. Y., Xu, L., Nabel, G. J., Crews, T. & Peters, C. J. (1998). Biochemical analysis of the secreted and virion glycoproteins of Ebola virus. *J. Virol.* **72**, 6442–6447.

6. Feldmann, H., Klenk, H. D. & Sanchez, A. (1993). Molecular biology and evolution of filoviruses. *Arch. Virol. Suppl.* **7**, 81–100.

7. Takada, A., Robison, C., Goto, H., Sanchez, A., Murti, K. G., Whitt, M. A. & Kawaoka, Y. (1997). A system for functional analysis of Ebola virus glycoprotein. *Proc. Natl Acad. Sci. USA*, **94**, 14764–14769.

8. Volchkov, V. E., Volchkova, V. A., Slenczka, W., Klenk, H. D. & Feldmann, H. (1998). Release of viral glycoproteins during Ebola virus infection. *Virology*, **245**, 110–119.

9. Wool-Lewis, R. J. & Bates, P. (1998). Characterization of Ebola virus entry by using pseudotyped viruses: identification of receptor-deficient cell lines. *J. Virol.* **72**, 3155–3160.

10. Maruyama, T., Rodriguez, L. L., Jahrling, P. B., Sanchez, A., Khan, A. S., Nichol, S. T. *et al.* (1999). Ebola virus can be effectively neutralized by antibody produced in natural human infection. *J. Virol.* **73**, 6024–6030.

11. Takada, A., Watanabe, S., Ito, H., Okazaki, K., Kida, H. & Kawaoka, Y. (2000). Downregulation of beta1 integrins by Ebola virus glycoprotein: implication for virus entry. *Virology*, **278**, 20–26.

12. Wilson, J. A., Hevey, M., Bakken, R., Guest, S., Bray, M., Schmaljohn, A. L. & Hart, M. K. (2000). Epitopes involved in antibody-mediated protection from Ebola virus. *Science*, **287**, 1664–1666.

13. Oswald, W. B., Geisbert, T. W., Davis, K. J., Geisbert, J. B., Sullivan, N. J., Jahrling, P. B. *et al.* (2007). Neutralizing antibody fails to impact the course of Ebola virus infection in monkeys. *PLoS Pathog.* **3**, e9.

14. Druar, C., Saini, S. S., Cossitt, M. A., Yu, F., Qiu, X., Geisbert, T. W. *et al.* (2005). Analysis of the expressed heavy chain variable-region genes of *Macaca fascicularis* and isolation of monoclonal antibodies specific for the Ebola virus soluble glycoprotein. *Immunogenetics*, 1–9.

15. Maruyama, T., Parren, P. W., Sanchez, A., Rensink, I., Rodriguez, L. L., Khan, A. S. *et al.* (1999). Recombinant human monoclonal antibodies to Ebola virus. *J. Infect. Dis.* **179**, S235–S239.

16. Yang, Z. Y., Duckers, H. J., Sullivan, N. J., Sanchez, A., Nabel, E. G. & Nabel, G. J. (2000). Identification of the Ebola virus glycoprotein as the main viral determinant of vascular cell cytotoxicity and injury. *Nat. Med.* **6**, 886–889.

17. Dildrop, R., Gause, A., Muller, W. & Rajewsky, K. (1987). A new V gene expressed in lambda-2 light chains of the mouse. *Eur. J. Immunol.* **17**, 731–734.

18. Sanchez, P. & Cazenave, P. A. (1987). A new variable region in mouse immunoglobulin lambda light chains. *J. Exp. Med.* **166**, 265–270.

19. Sanchez, P., Marche, P. N., Le Guern, C. & Cazenave, P. A. (1987). Structure of a third murine immunoglobulin lambda light chain variable region that is expressed in laboratory mice. *Proc. Natl Acad. Sci. USA*, **84**, 9185–9188.

20. Sanchez, P., Marche, P. N., Rueff-Juy, D. & Cazenave, P. A. (1990). Mouse V lambda X gene sequence generates no junctional diversity and is conserved in mammalian species. *J. Immunol.* **144**, 2816–2820.

21. Galin, F. S., Maier, C. C., Zhou, S. R., Whitaker, J. N. & Blalock, J. E. (1996). Murine V lambda X and V lambda x-containing antibodies bind human myelin basic protein. *J. Clin. Invest.* **97**, 486–492.

22. Maier, C. C., Galin, F. S., Jarpe, M. A., Jackson, P., Krishna, N. R., Gautam, A. M. *et al.* (1994). A V lambda x-bearing monoclonal antibody with similar specificity and sequence to encephalitogenic T cell receptors. *J. Immunol.* **153**, 1132–1140.

23. Li, P., Huey-Tubman, K. E., Gao, T., Li, X., West, A. P., Jr, Bennett, M. J. & Bjorkman, P. J. (2007). The structure of a polyQ–anti-polyQ complex reveals binding according to a linear lattice model. *Nat. Struct. Mol. Biol.* **14**, 381–387.

24. Al-Lazikani, B., Lesk, A. M. & Chothia, C. (1997). Standard conformations for the canonical structures of immunoglobulins. *J. Mol. Biol.* **273**, 927–948.

25. DeLano, W. L. (2002). The PyMol Molecular Graphics System, DeLano Scientific, Palo Alto, CA, USA.

26. Stanfield, R. L., Zemla, A., Wilson, I. A. & Rupp, B. (2006). Antibody elbow angles are influenced by their light chain class. *J. Mol. Biol.* **357**, 1566–1574.

27. Huang, M., Syed, R., Stura, E. A., Stone, M. J., Stefanko, R. S., Ruf, W. *et al.* (1998). The mechanism of an inhibitory antibody on TF-initiated blood coagulation revealed by the crystal structures of human tissue factor, Fab 5G9 and TF, G9 complex. *J. Mol. Biol.* **275**, 873–894.

28. Stanfield, R. L., Takimoto-Kamimura, M., Rini, J. M., Profy, A. T. & Wilson, I. A. (1993). Major antigen-induced domain rearrangements in an antibody. *Structure*, **1**, 83–93.

29. Chothia, C. & Lesk, A. M. (1987). Canonical structures for the hypervariable regions of immunoglobulins. *J. Mol. Biol.* **196**, 901–917.

30. Martin, A. C. & Thornton, J. M. (1996). Structural families in loops of homologous proteins: automatic classification, modelling and application to antibodies. *J. Mol. Biol.* **263**, 800–815.

31. Wu, S. & Cygler, M. (1993). Conformation of complementarity determining region L1 loop in murine IgG lambda light chain extends the repertoire of canonical forms. *J. Mol. Biol.* **229**, 597–601.

32. Tomlinson, I. M., Cox, J. P. L., Gherardi, E., Lesk, A. M. & Chothia, C. (1995). The structural reper-

toire of the human V kappa domain. *EMBO J.* **14**, 4628–4638.

33. Stanfield, R. L., Gorny, M. K., Williams, C., Zolla-Pazner, S. & Wilson, I. A. (2004). Structural rationale for the broad neutralization of HIV-1 by human monoclonal antibody 447-52D. *Structure*, **12**, 193–204.

34. Stanfield, R. L., Gorny, M. K., Zolla-Pazner, S. & Wilson, I. A. (2006). Crystal structures of human immunodeficiency virus type 1 (HIV-1) neutralizing antibody 2219 in complex with three different V3 peptides reveal a new binding mode for HIV-1 cross-reactivity. *J. Virol.* **80**, 6093–6105.

35. Rudolph, M. G., Stanfield, R. L. & Wilson, I. A. (2006). How TCRs bind MHCs, peptides, and coreceptors. *Annu. Rev. Immunol.* **24**, 419–466.

36. Fersht, A. R., Shi, J. P., Knill-Jones, J., Lowe, D. M., Wilkinson, A. J., Blow, D. M. *et al.* (1985). Hydrogen bonding and biological specificity analysed by protein engineering. *Nature*, **314**, 235–238.

37. Centers for Disease Control and Prevention. (1995). Outbreak of Ebola Viral Hemorrhagic Fever—Zaire. *Morbid. Mortal. Wkly. Rep.* **44**, 381–382.

38. Centers for Disease Control and Prevention. (1995). Update: outbreak of Ebola viral hemorrhagic fever. *Morbid. Mortal. Wkly. Rep.* **44**, 399.

39. Ksiazek, T. G., Rollin, P. E., Williams, A. J., Bressler, D. S., Martin, M. L., Swanepoel, R. *et al.* (1999). Clinical virology of Ebola hemorrhagic fever (EHF): virus, virus antigen, and IgG and IgM antibody findings among EHF patients in Kikwit, Democratic Republic of the Congo. *J. Infect. Dis.* **179**, S177–S187.

40. Sanchez, A., Khan, A. S., Zaki, S. R., Nabel, G. J., Ksiazek, T. G. & Peters, C. J. (2001). *Filoviridae*: Marburg and Ebola viruses. In *Fields Virology* (Knipe, D. M. & Howley, P. M., eds), pp. 1279–1304, Lippincott, Williams, and Wilkins, Philadelphia.

41. Tsurushita, N., Hinton, P. R. & Kumar, S. (2005). Design of humanized antibodies: from anti-Tac to Zenapax. *Methods*, **36**, 69–83.

42. Pflugrath, J. W. (1999). The finer things in X-ray diffraction data collection. *Acta Crystallogr., Sect. D: Biol. Crystallogr.* **55**, 1718–1725.

43. Adams, P. D., Pannu, N. S., Read, R. J. & Brünger, A. T. (1997). Cross-validated maximum likelihood enhances crystallographic simulated annealing refinement. *Proc. Natl Acad. Sci. USA*, **94**, 5018–5023.

44. Brünger, A. T., Adams, P. D., Clore, G. M., DeLano, W. L., Gros, P., Grosse-Kunstleve, R. W. *et al.* (1998). Crystallography & NMR system: a new software suite for macromolecular structure determination. *Acta Crystallogr., Sect. D: Biol. Crystallogr.* **54**, 905–921.

45. McRee, D. M. (1993). *Practical Protein Crystallography*, Academic Press, San Diego, CA.

46. Brunger, A. T., Krukowski, A. & Erickson, J. W. (1990). Slow-cooling protocols for crystallographic refinement by simulated annealing. *Acta Crystallogr., Sect. A*, **47**, 195–204.

47. Adams, P. D., Gopal, K., Grosse-Kunstleve, R. W., Hung, L. W., Ioerger, T. R., McCoy, A. J. *et al.* (2004). Recent developments in the PHENIX software for automated crystallographic structure determination. *J. Synchrotron Radiat.* **11**, 53–55.

48. Adams, P. D., Grosse-Kunstleve, R. W., Hung, L. W., Ioerger, T. R., McCoy, A. J., Moriarty, N. W. *et al.* (2002). PHENIX: building new software for automated crystallographic structure determination. *Acta Crystallogr., Sect. D: Biol. Crystallogr.* **58**, 1948–1954.

49. Afonine, P. D., Grosse-Kunstleve, R. W. & Adams, P. D. (July, 2005). The Phenix refinement framework. *CCP4 Newsl.* Contribution 8.

50. Winn, M. D., Isupov, M. N. & Murshudov, G. N. (2001). Use of TLS parameters to model anisotropic displacements in macromolecular refinement. *Acta Crystallogr., Sect. D: Biol. Crystallogr.* **57**, 122–133.

51. Ye, Y. & Godzik, A. (2003). Flexible structure alignment by chaining aligned fragment pairs allowing twists. *Bioinformatics*, **19**, ii246–ii255.

52. Lawrence, M. C. & Colman, P. M. (1993). Shape complementarity at protein/protein interfaces. *J. Mol. Biol.* **234**, 946–950.

53. Berman, H. M., Westbrook, J., Feng, Z., Gilliland, G., Bhat, T. N., Weissig, H. *et al.* (2000). The Protein Data Bank. *Nucleic Acids Res.* **28**, 235–242.